

# GAMMA-RAYS FROM SUPERNOVA REMNANTS AND THE SIGNATURES OF DIFFUSIVE SHOCK ACCELERATION

Matthew G. Baring,<sup>1†</sup> Donald C. Ellison<sup>2</sup> and Isabelle Grenier<sup>3</sup>

<sup>1</sup>Lab. for High Energy Astrophysics, NASA Goddard Space Flight Center, Greenbelt, MD 20771, U.S.A.

<sup>2</sup>Department of Physics, Box 8202, North Carolina State University, Raleigh NC, 27695, U.S.A.

<sup>3</sup>EUROPA-Université Paris, Paris VII and DAPNIA/Service d'Astrophysique, CE-Saclay, Gif/Yvette, France

†Compton Fellow, Universities Space Research Association

## ABSTRACT

While the definitive detection of gamma-rays from known supernova remnants (SNRs) remains elusive, the collection of unidentified EGRET sources that may be associated with SNRs has motivated recent modelling of TeV emission from these sources. Current theoretical models use power-law shock-accelerated protons and electrons in their predictions of expected gamma-ray TeV fluxes from those unidentified EGRET sources with remnant associations. In this paper, we explore a more detailed non-linear shock acceleration model, which generates non-thermal proton distributions and includes a self-consistent determination of shock hydrodynamics. We obtain gamma-ray spectra for SNRs allowing for the cessation of acceleration to high energies that is due to the finite ages and sizes of remnants. Gamma-ray spectral cutoffs can be observed in the TeV range for reasonable remnant parameters, and deviations from power-law behaviour are found at all energies ranging from 1 MeV up to the cutoff. Correlated observations by INTEGRAL, Whipple and other instruments may provide stringent constraints to our understanding of supernova remnants.

**Keywords:** supernova remnants; gamma-rays; diffusive shock acceleration.

## 1. INTRODUCTION

Supernova remnants have long been invoked as a principal source of galactic cosmic rays, created via the process of diffusive Fermi acceleration at their expanding shock fronts (e.g. Drury 1983, Lagage and Cesarsky 1983, Blandford and Eichler 1987). Such systems can also provide gamma-ray emission via the interaction of the cosmic ray population with the ambient remnant environment; this concept was explored recently by Drury, Aharonian and Völk (1994). In their model, the gamma-ray luminosity is spawned by collisions between the cosmic rays and nuclei from the ambient SNR environment. Inverse Compton scattering involving shock-accelerated  $e^-$  and the cosmic microwave background and also IR/optical emission (from dust/starlight) forms added components in the  $\gamma$ -ray SNR models of De Jager and Mastichiadis

(1996) and Gaisser, Protheroe and Stanev (1996).

Given the absence of definitive detections of gamma-rays from known supernova remnants, the motivation for modelling these “hypothetical” sources hinges on over a dozen spatial associations of unidentified EGRET sources at moderately low galactic latitudes with well-studied radio SNRs. These include IC 443,  $\gamma$  Cygni and W44, and many have neighbouring dense environments, which seem essential in order to provide sufficient gamma-ray luminosity to exceed EGRET’s sensitivity threshold. Confirmation of these associations will probably only come with better gamma-ray angular resolution (e.g. at the soft gamma-ray band addressed by the INTEGRAL mission) and/or positive TeV detections. The remnants associated with several of the EGRET unidentified sources show an apparently low level of TeV emission, as determined by Whipple (Lessard et al. 1995), which may be marginally inconsistent with the spectra generated in the model of Drury, Aharonian and Völk (1994); Gaisser, Protheroe and Stanev (1996) use a slightly steeper accelerated proton distribution to provide greater consistency between the EGRET and Whipple bands. De Jager and Mastichiadis (1996) suggest that there may be an intrinsic cutoff in the SNR-generated cosmic ray population that would spawn a complete absence of TeV emission, which is quite compatible with the data.

All of the above models invoke simple power-law accelerated particle populations. In this paper, we utilize the more sophisticated output of shock acceleration simulations (e.g. Jones and Ellison 1991) to address the issues of spectral curvature and the maximum energy of acceleration in the context of SNR gamma-ray emission. We use output from the fully non-linear Monte Carlo simulations of Ellison and Reynolds (1991) and Ellison, Baring and Jones (1996) to describe the accelerated population in environments where it influences the dynamics of the SNR shell. Such non-linear effects are crucial to the modelling of gamma-ray emission in SNRs. Our results make clear predictions of what maximum energies of gamma-rays are expected, and further make more accurate determinations of the level of TeV emission relative to the MeV range in these sources. We find that the TeV/GeV flux ratio in our non-linear regime is reduced by factors of a few below pure power-law proton scenarios, a result that is very important for correlated observations by INTEGRAL, Whipple and other gamma-ray instruments.

## 2. FERMI ACCELERATION AT SHOCKS

Diffusive shock acceleration is usually assumed to generate power-law particle populations in astrophysical models. This simple approximation omits the effect the accelerated particles themselves have on the hydrodynamics of their shocked environment. Considerations of such non-linear dynamics are essential to the gamma-ray SNR problem since the peak luminosity arises at the onset of the Sedov phase (Drury, Aharonian and Völk 1994) where the fraction of ram pressure going into cosmic rays and nonlinear effects are maximized. These non-linear effects, well-documented in the reviews of Drury (1983) and Jones and Ellison (1991), have a feedback on the acceleration mechanism and its efficiency. This becomes evident when it is observed that the “test-particle” power-law slope depends purely on the compression ratio of flow speeds on either side of the shock, and that this ratio is ultimately dependent on the hydrodynamics.

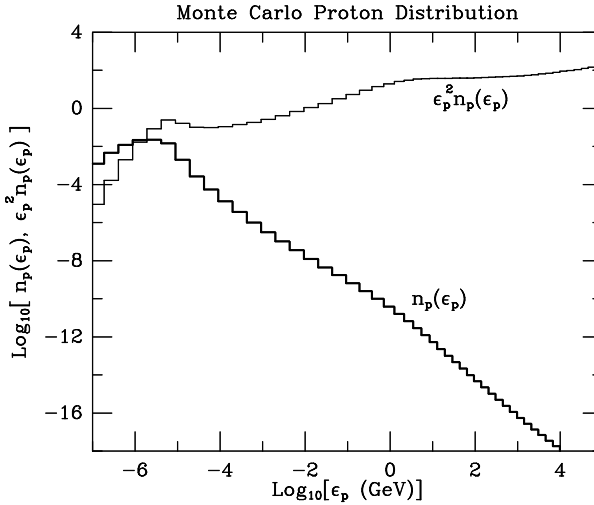


*Figure 1:* A typical proton distribution  $n_p(\epsilon_p)$ , of arbitrary normalization, resulting from Monte Carlo simulations of particle acceleration at SNR shocks. The transition to relativistic energies produces a “bump” at around the kinetic energy  $\epsilon_p \sim 1$  GeV, a result of assuming a momentum-dependent mean free path. The  $\epsilon_p^2 n_p(\epsilon_p)$  representation gives a good feel for the spectral curvature produced by the non-linear hydrodynamics above 1 GeV.

Our Monte Carlo simulation of Fermi acceleration determines the acceleration efficiency and maximum energy of acceleration. Although steady-state, this method can roughly mimic the net features of the time dependence of the SNR expansion and may describe the general spectral properties quite well just prior to the start of the Sedov phase. A typical proton distribution is shown in Fig. 1. Positive curvature appears in the distribution above 1 GeV due to the non-linear effects. The difference in slopes about the proton rest mass energy at  $\sim 1$  GeV is just due to the varying dependence of momentum on energy as prescribed by special relativity. The pressure of the accelerated population acts to slow down the fast-moving flow upstream of the shock.

High-momentum protons have longer mean-free paths  $\lambda$ , a model assumption that is supported by observations made by plasma experiments at the Earth’s bow shock (e.g. Ellison, Möbius and Paschmann 1990), and therefore typically influence the flow on larger scalelengths.

The maximum compression ratio is achieved at the largest scales, i.e. farthest from the downstream region (inside of the SNR shell; see Ellison, Baring and Jones 1996 for typical velocity profiles), implying an increased efficiency of accelerating higher-energy particles relative to those at lower energies. Upward spectral curvature ensues, and this has a significant influence on predictions of TeV fluxes in gamma-ray SNRs. Non-linear predictions of the spectral index differ significantly from the test-particle case (Ellison, Baring and Jones 1996); in Fig. 1, a  $p^{-2}$  proton momentum distribution from a strong shock would be flat (i.e. horizontal) above 1 GeV in the  $\epsilon_p^2 n_p(\epsilon_p)$  representation. Deviations from a power-law behaviour can be up to a factor of around 3 over four decades in particle energy in the 1 GeV – 10 TeV range. Such enhancements are extremely important for discussion of the potential observability of EGRET sources by Whipple, HEGRA and other ground-based TeV experiments.

### 2.1. The maximum particle energy

The maximum energy of Fermi-accelerated protons is determined by two considerations, namely the acceleration time vs. the age of the remnant, and the diffusive scale-length of the particles vs. the size of the ionized region. For test-particle shocks (i.e. linear ones that produce power-law protons), the acceleration timescale (e.g. see Forman and Morfill 1979, Drury 1983 for derivations) for the Fermi mechanism at plane-parallel shocks up to energy  $E_{\text{TeV}}$  (in units of TeV), far above the injection energy, can be written as

$$\tau_a = 31.7 \frac{\eta}{QB_{-5}} \frac{r(r+1)}{r-1} \frac{E_{\text{TeV}}}{u_{1000}^2} \text{ yr}, \quad (1)$$

where  $r = u_{\text{ups}}/u_{\text{down}}$  is the compression ratio,  $B_{-5}$  is the field in units of  $10^{-5}$  Gauss, and  $\eta$  is the ratio of the particle mean free path  $\lambda$  to its gyroradius  $r_g$ . Here  $Q$  is the charge number of the ion (e.g.  $Q = 1$  for protons and  $Q = 2$  for alpha particles). Eq. (1) is a specialization of Eq. (4) of Ellison, Baring and Jones (1995), expressed in units appropriate to the SNR problem at hand. Quite generally,  $\eta \geq 1$  and one infers values of  $1 < \eta < 10$  in interplanetary shocks in the inner heliosphere (Baring et al. 1997). Shock speeds  $u_{1000}$  ( $= u_{\text{ups}}$ ) are in units of 1000 km/s. Implicit in such a formula is the assumption that the mean free path scales as  $\lambda \propto r_g \propto p$ , which seems reasonable in the light of the aforementioned observations of plasmas in the heliosphere. Although Eq. (1) is strictly confined to test-particle regimes, it serves also as an order-of-magnitude estimate for the full non-linear problem that is treated by the Monte Carlo simulation. Assume that the age of remnants is just their shell radii, typically in the vicinity of a few pc, divided by the expansion speed  $u_{1000}$ . This contention can be modified by the dynamical interaction of the supernova ejecta with the ISM, leading to larger age estimates (e.g. Chevalier 1982). For SN Ia, typically  $u_{1000} \sim 10$ , while for the more-massive ejecta associated with SN II, the shock speed is slower:  $u_{1000} \sim 4$ . Hence (bright) remnant ages are typically  $1 - 10 \times 10^{10}$  sec, implying age-limited acceleration terminating at around  $10^4 - 10^5$  GeV.

The diffusion scale of the SNR medium is  $\kappa/u$  for a diffusion coefficient of  $\kappa = \lambda v/3$ . Hence the diffusion scale

(in parsecs) is comparable to

$$d_{\text{pc}} = 3 \times 10^{-2} \frac{\eta}{QB_{-5}} \frac{E_{\text{TeV}}}{u_{1000}} . \quad (2)$$

For acceleration regions of the order of a tenth of the shell size (much smaller might be expected for remnants in the neighbourhood of dense neutral regions, which is frequently the case for remnants associated with unidentified EGRET sources), size-limited acceleration terminates also at around  $10^4$ – $10^5$  GeV. The factor of a tenth represents an estimate of the effective escape lengthscale taking into account shell geometry and the remnant history. Note that if the acceleration time in Eq. (1) is multiplied by the shock speed, the resulting length scale is of the order of Eq. (2), differing only by factors involving the compression ratio. This is not surprising since both estimates have their origin in particle diffusion. Clearly higher compression ratios will enhance the acceleration time, defining the general property that stronger shocks usually produce size-limited rather than time-limited maximum energies of acceleration. Another important property of these estimates is that Eqs. (1) and (2) depend on the charge of the species but not explicitly on the mass. Hence electrons potentially have similar maximum energies to protons if cooling is absent, while helium and heavier nuclei with higher charge states can be accelerated to higher energies (as opposed to energy per nucleon).

### 3. GAMMA-RAY EMISSION SPECTRA

The effects of using the full non-linear Monte Carlo simulation for predicting gamma-ray emissivities from SNRs can be adequately demonstrated using just the  $\pi^0$  emission component. Treatment of other radiation mechanisms (discussed below) is deferred to future work, in part because the hadronic contributions tend to provide the major portion of the gamma-ray radiation. The  $\pi^0$  emissivity and spectrum were calculated much along the lines of the work of Dermer (1986):  $pp$  collisions produce  $\pi^0$ s, which subsequently decay to produce two photons. The proton component of the cosmic rays collides with nuclei in the cold ambient ISM; note that cosmic rays of higher mass number also contribute significantly to the  $\pi^0$  emissivity. Low-energy protons, typically with kinetic energies below a few GeV, create pions via the  $\Delta$  resonance, following the model of Stecker (1970). As their energy increases, more resonances are sampled. High energy protons, typically above 10 GeV, interact according to a radial scaling empirical formalism (e.g. Tan and Ng 1983). Details of these formalisms, kinematics and numerical procedure, can be found in Baring and Stecker (1997, in preparation). Note that the gamma-ray spectral profiles for different cosmic ray proton kinetic energies are symmetric about the energy  $m_\pi c^2/2$ , due to the pion decay kinematics (e.g. Stecker 1970).

Fig. 2 shows various representations of a  $\pi^0$  gamma-ray spectrum resulting from a proton distribution generated by the non-linear Monte Carlo simulation. In this case, protons are accelerated out to a few tens of TeV, a limit obtainable from Eq. (1) for a very young remnant with  $\eta \sim 10$  and  $r \sim 11$  (it must be remembered that non-linear shocks generate overall compression ratios much larger than 4; see Jones and Ellison 1991; Ellison, Baring and Jones 1996). The differential

photon spectrum is largely visually uninteresting, so integral and double-integral (“ $\nu F_\nu$ ”) spectra are plotted to highlight the spectral properties. One prominent feature is that spectra flatter than  $\varepsilon_\gamma^{-2}$  result. The spread induced by the kinematic phase space for pion production and decay tends to smear out the underlying curvature of the proton population. Yet, for comparison, the integral spectrum resulting from a power-law proton population with a high-energy cutoff is depicted in Fig. 2, indicating that it overestimates the TeV/EGRET flux ratio by a factor of a few. This clearly yields an indication of the improvement of the non-linear calculation over the standard test-particle  $p^{-2}$  infinite power-law case considered by Drury, Aharonian and Völk (1994, and also approximately by Gaisser, Protheroe and Stanev 1996). Therefore it follows that these test-particle implementations of shock acceleration theory can significantly over-predict the TeV/EGRET flux ratio. Consequently, the incorporation of non-linear dynamical considerations can potentially relax observational constraints imposed by the Whipple upper limits to IC443, W28 and  $\gamma$ -Cygni as presented by Lessard et al. (1995). Note that the spectral structure below 1 GeV in the proton distribution in Fig. 1 is immaterial since such kinetic energies are below the  $\pi^0$  production threshold.

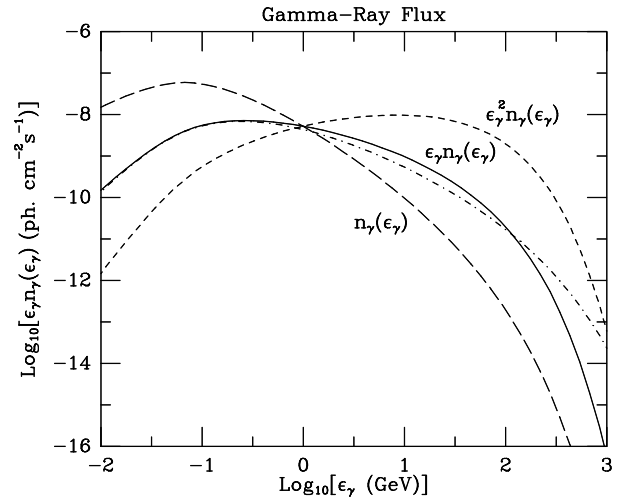


Figure 2: The  $\gamma$ -ray flux at earth, for a young SNR about a kpc distant, integrated over a shock acceleration produced proton distribution (long dashed lines). The solid curve represents the integral spectrum for this distribution, and the dash-dot curve the integral spectrum from a pure power-law ( $p^{-2}$ ) proton population (exponentially cutoff at around 1 TeV) with index given by the low energy portion of the non-linear model proton distribution. The  $\varepsilon_\gamma^2 n_\gamma$  representation clearly illustrates the effects of spectral curvature and the cutoff.

DeJager and Mastichiadis (1996) suggested that constraints to the TeV/EGRET flux ratio can be relieved by having the photon spectrum turn over below the Whipple sensitivity threshold. The maximum energies of the protons at  $\sim 10$ – $30$  TeV propagates down into the few TeV range in the gamma-ray spectrum due to the inelasticity of the  $pp \rightarrow pp\pi^0 \rightarrow pp\gamma\gamma$  chain. Hence for the illustrated case, HEGRA would be unlikely to see an EGRET source, but Whipple potentially could. Turnovers at such low energies are predicted neither in the work of Gaisser, Protheroe and Stanev (1996), nor by Drury, Aharonian and Völk (1994), mainly because they focus on cooling-limited rather than age/size-limited acceleration. Their inverse Compton cooling rates off the microwave and local

IR backgrounds turn out to be low enough that the freely expanding shell purely defines the maximum proton energy. The non-linear shock acceleration solution treated here provides natural cutoffs in the TeV range that can also yield compatibility with the Whipple upper limits for the appropriate choice of remnant shock parameters. By inspection of Eq. (2), slightly lower shock speeds can suppress emission in the TeV range, which may well be necessary to explain the four orders of magnitude difference in integral flux inferred for  $\gamma$ -Cyggni (see Lessard et al. 1995) between 100 MeV and 500 GeV from the EGRET source flux and the Whipple upper limits. The implication of such low maximum energies for cosmic ray protons is naturally that older SNRs are required to produce the bulk of cosmic rays out to the  $10^{14}$ eV “knee,” so that gamma-ray SNRs are a gamma-ray bright minority of the cosmic ray-producing remnant population.

#### 4. DISCUSSION

Generalizing beyond  $\pi^0$  emission generated via  $pp$  collisions is clearly important. These interactions also spawn charged pions at comparable rates, and these yield secondary electrons and positrons and consequently inverse Compton emission as discussed in Gaisser, Protheroe and Stanev (1996). While the  $\pi^0$  decay spectrum traces the proton distribution, the inverse Compton spectrum is potentially much flatter due to the kinematics. Hence, in principal, the inverse Compton mechanism can be much more efficient at higher energies, and perhaps dominate the  $\pi^0$  decay products; such scenarios are discussed in the context of the diffuse galactic gamma-ray background by Hunter et al. (1996). Primary shock-accelerated electrons are in principle possible, though the theoretical efficiency of their generation is very poorly understood. Gaisser, Protheroe and Stanev (1996) argue that the EGRET/Whipple spectral constraints for IC 443 imply that inverse Compton emission is relatively unimportant and also that the primary electron population is of low abundance. Within the confines of non-linear shock acceleration theory, unlike the power-law choices made (i.e. linear shock models) by Gaisser, Protheroe and Stanev (1996) and De Jager and Mastichiadis (1996), the accelerated electron spectrum does not trace the proton distribution at all energies. Below a few GeV, the electron diffusion lengths are always less than those of protons of comparable energy, so that electrons effectively experience a weaker portion of the shock structure than do the protons (e.g. see Ellison and Reynolds 1991 for a discussion). The net effect is that the electron distributions are steeper below a few GeV and the population level above a few GeV much lower than is predicted in the linear shock models. Therein lies another crucial aspect of the inclusion of the non-linear effects of shock acceleration theory: the linear approaches cited above seriously overestimate the efficiency of electron acceleration, and hence the contribution of the inverse Compton and bremsstrahlung processes to the SNR luminosity. Such issues will be dealt with in a future paper (Baring et al. 1997, in preparation).

The issue of the prominence or otherwise of an inverse Compton component may well be elucidated by coordinated observations at the TeV range and by INTEGRAL at MeV energies: the  $\pi^0$  decay channel produces much lower emissivity below  $m_{\pi}c^2/2 \sim 67$  MeV due to decay kinematics, so that an inverse Compton spectrum can be much more visible in the soft gamma-ray regime. An

asset of INTEGRAL will be its angular-resolution capability (e.g. see Winkler 1996). EGRET has difficulty resolving on scales of the order of the angular diameter of nearby remnants; hence it is not clear whether any detected gamma-ray emission is associated with whole remnants, portions or “hot spots” (or neither). Improved angular resolution at MeV and TeV energies will clearly pin down or disprove these associations. Note also that, apart from protons, heavier nuclei make up the cosmic ray population and the ambient ISM, and these also contribute significantly to the gamma-ray and electronic products; their inclusion in our gamma-ray emissivity calculations is deferred to future work. In conclusion, coupled TeV/sub-GeV observations of supernova remnants, in which the INTEGRAL can play a big role, will discriminate between various gamma-ray emission models of these sources, and enhance our understanding of the cosmic ray production. The non-linear effects described here are an essential ingredient for any model that invokes Fermi acceleration at SNRs, particularly since their prediction of enhanced TeV/GeV flux ratios can tighten model constraints imposed by current TeV upper limits and possible future detections.

#### ACKNOWLEDGMENTS

We thank S. Reynolds and P. Goret for many helpful and informative discussions.

#### REFERENCES

- Baring, M. G., Ogilvie, K. W., Ellison, D. C. and Forsyth, R. J.: 1997 *Ap. J.* in press.
- Blandford, R. D. and Eichler, D.: 1987 *Phys. Rep.* **154**, 1
- Chevalier, R.: 1982 *Ap. J.* **258**, 790
- De Jager, O. & Mastichiadis, A.: 1996 preprint.
- Dermer, C. D.: 1986 *Astron. Astr.* **157**, 223
- Drury, L. O'C: 1983 *Rep. Prog. Phys.* **46**, 973
- Drury, L. O'C., Aharonian, F. A., and Völk, H. J.: 1994 *Astron. Astr.* **287**, 959
- Ellison, D. C., Baring, M. G. and Jones, F. C.: 1996 *Ap. J.* **453**, 873
- Ellison, D. C., Baring, M. G. and Jones, F. C.: 1996 *Ap. J.* in press.
- Ellison, D. C., Möbius, E. and Paschmann, G.: 1990 *Ap. J.* **352**, 376
- Ellison, D. C. and Reynolds, S. J.: 1991 *Ap. J.* **382**, 242
- Forman, M. A. and Morfill, G.: 1979 *Proc. 16th ICRC (Kyoto)*, Vol V, p. 328.
- Gaisser, T. K., Protheroe, R. J. and Stanev, T.: 1996 *Ap. J.* submitted.
- Hunter, S. D., et al.: 1996 *Ap. J.* submitted.
- Jones, F. C. and Ellison, D. C.: 1991 *Space Sci. Rev.* **58**, 259
- Lagage, P. O., and Cesarsky, C. J.: 1983 *Astron. Astr.* **125**, 249
- Lessard, R. W., et al.: 1995 *Proc. 24th ICRC (Rome)*, Vol II, p. 475.
- Stecker, F. W.: 1970 *Cosmic Gamma Rays*, (NASA, SP-249).
- Tan, L. C. & Ng, L. K.: 1983 *J. Phys. G: Nucl. Phys.* **9**, 1289

